Independently controllable single-input dual-output DC-DC converter for DC microgrid based PV fed EV charging stations

2024 IEEE 4th International Conference on Sustainable Energy and Future Electric Transportation (SEFET) | 979-8-3503-8399-7/24/$31.00 ©2024 IEEE | DOI: 10.1109/SEFET61574.2024.10718259

Maya Vijayan
Dept. of Electrical and Electronics Engg.
SRM University,AP
India
0000-0001-7745-026X

Ramanjaneya Reddy U
Dept. of Electrical and Electronics Engg.
SRM University,AP
India
0000-0002-9176-2558

Tarkeshwar Mahto
Dept. of Electrical & Electronics Engg.
SRM University,AP
India
0000-0001-7643-740X

Narasimharaju B L
Dept. of Electrical Engineering,
National Institute of Technology
Warangal, India
0000-0002-3033-5712

Raveendhra Dogga
Dept of Electrical Engineering,
MNIT Allahabad
Prayagraj, India
0000-0003-1013-4881

***Abstract*—A new non-isolated single-input dual-output (NI-SIDO) DC-DC converter is proposed in this paper. The converter has the advantage of incorporating multiple outputs for energy storage applications, applicable in DC micro-grid storage systems, Electric vehicular charging stations, battery converters, and renewable energy systems without a filter capacitor. The significant advantage of the converter is it uses the interleaving technique to incorporate the outputs. The voltage stress across the switches and capacitor voltage stress is also reduced drastically. Thus it reduces the capacitor size when compared with the conventional boost converter. A closed-loop control strategy is implemented to control the load voltage as well as the inductor current. The converter is designed, analyzed, implemented, and tested using MATLAB SIMULINK software for 150W. The Simulation results are presented under various operating conditions such as changes in load with solar PV systems. The results from real-time testing are presented with the OPAL-RT system.**

***Index Terms*—Dual-output converter, Single-inductor converter, Solar PV converter, Electric Vehicles, Battery storage systems, Single-input dual-output converter, Interleaved converter.**

I. INTRODUCTION

In recent years, the requirement for green energy has increased, which triggered the research on renewable and sustainable energy sources such as solar Photovoltaic, fuel-cell, wind energy, battery storage, supercapacitors, etc [1]–[4]. Distributed generation system is admirable as it has better flexibility, reliability, and control, which is widely acceptable for applications such as Electric Vehicles (EV), DC micro-grids, Energy storage, and Lighting [5]–[7]. For the abovementioned applications, with consideration of performance and cost optimization, bidirectional multi-port converters are advantageous over conventional single-input single-output converters [8]. Bidirectional converters are widely adopted for battery charging/discharging applications [9], for applications in EVs and hybrid energy storage systems. This may reduce the number of converters required for multiple energy sources, with a wide range of voltage ratings with a single inductor [10], [11]. DC-DC converter variants are classified as isolated and non-isolated topologies. The transformer isolation is the basis of the classification. Isolated converters with transformers are bulky, such that they are less preferred for major applications [11], [12].

Traditional converters adjust their output voltage using a single control parameter known as the duty cycle. Nevertheless, employing multiple converters with distinct control systems leads to increased power components, resulting in reduced reliability and efficiency [13].

To address the abovementioned challenges, multi-output DC-DC converters have been introduced recently [13]–[15]. Non-isolated multi-output converters are an alternative to such applications that don't require galvanic isolation which maintains higher efficiency and space-optimized [16]. Similarly, single switch-based and multi-switched multi-output converters are also available in literature [17], [18].

Numerous multi-output DC-DC converters have been proposed in the existing literature [19], [21]. There are direct approaches to acquire multi-outputs from a single sourced single variable-controlled converters [20]. Reference [19] proposes a single inductor multi-port converter, which is flexible and can aid decentralised power between various sources.

Fig. 1 represents the schematic of the application of bidirectional multi-port converters on DC microgrids.
The proposed converter is a single-input dual-output DC-DC converter with Solar PV as the input source. In the paper boost mode of operation is presented. The converter consists of an LC tank circuit. There are two outputs, which are parallel in operation and the converter can operate at a

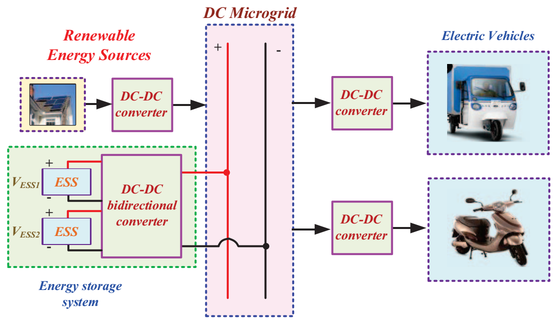

Fig. 1. Schematic of DC micro-grid with Bidirectional multi-port converter.

wide range of voltages. The advantage of the converter is its capability of multiple outputs for energy storage applications. Its compactness helps in the wide use of EVs. The feature of the proposed converter is a dual-output capability for battery energy storage applications like EVs, Hybrid energy storage systems in DC micro-grids, etc. It is capable of increasing the output ports as desired. The reduced capacitor voltage is another peculiarity of the proposed converter. The switches operate complementary, so the control is simple.

The paper is organised as: Section 2 is the proposed converter and its operation, and analysis, Section 3 deals with the results and discussion, paper concludes in Section 4.

II. Proposed Converter

The proposed NI-SIDO converter topology is shown in Fig. 2a. The topology is an advancement of the single inductor SISO system which consists of an interleaved converter. The converter consists of active switches, S_a, S_b, S_c, S_d, and LC circuits. The operation of the converter in both the forward directions can be controlled by the switching pulses. The converter consists of two output ports for energy storage applications such as EV charging and battery charging. In the on-period of the switch, the two inductors are magnetized by the source. Then, in the off-period, the inductors demagnetize to the load in parallel. The converter is engineered with the goal of minimizing voltage stresses on the capacitor. The primary role of the inductor is to accumulate energy during the "on" phase of the converter and then discharge this stored energy during the "off" phase of the primary switch. Furthermore, the inductor serves to mitigate the current ripple. Another component for storing energy, the capacitor, is employed to smooth out voltage fluctuations in both scenarios: in the conventional SIDO converter (Boost-Converter) and the proposed NI-SIDO converter. Indeed, during the boost operation, the primary switches, S_b and S_d, assume the role of the main switches and operate at the switching frequency. Conversely, D_{sa} and D_{sc} function as freewheeling diodes within this configuration.

A. Modes of operation

Figures 2 and 3 depict the equivalent circuit and idealized waveforms for the NI-SIDO converter operating in boost

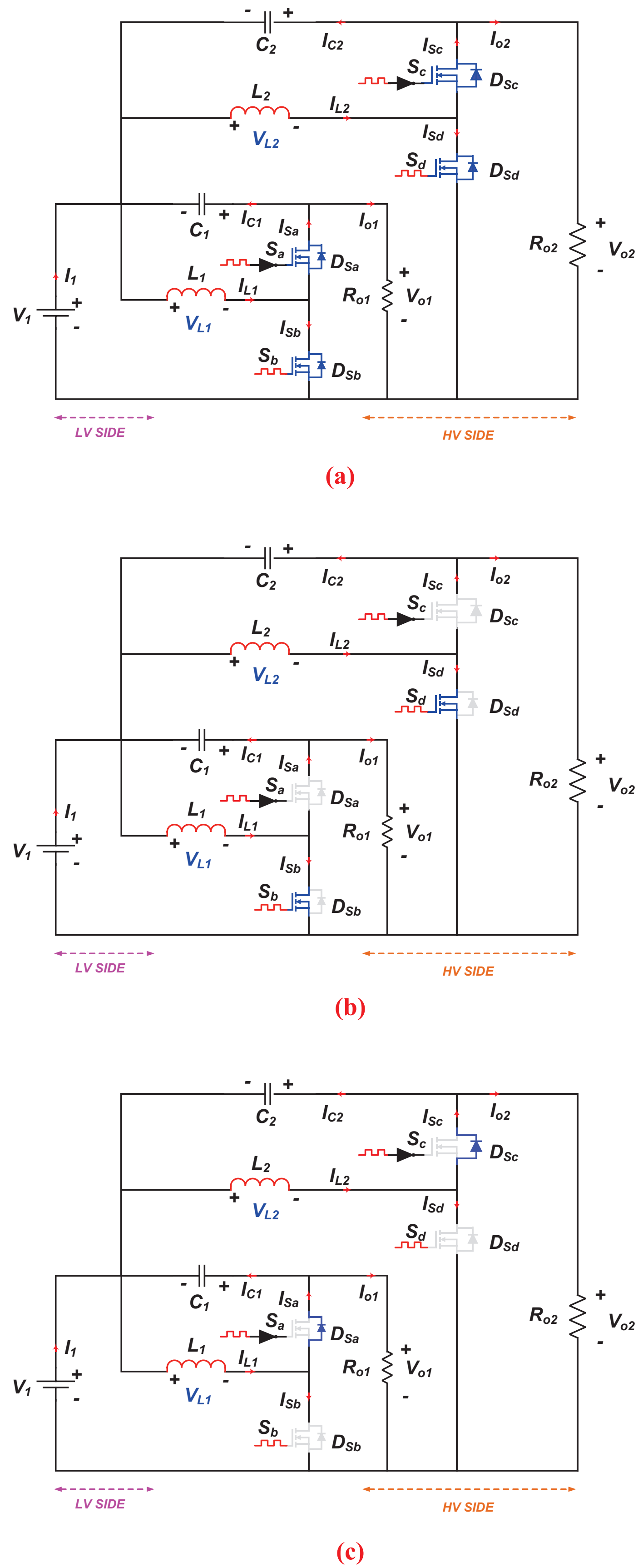

Fig. 2. Schematic of DC microgrid with NI-SIDO converter.

mode, respectively. The converter switch S_b and S_d is turned on and off during the boost mode of operation. In this mode, the switch S_a and S_c is off and the diode of MOSFET, D_{sa} and D_{sc}, operates. The boost mode, which is based on the switching there are 2 modes of operation.

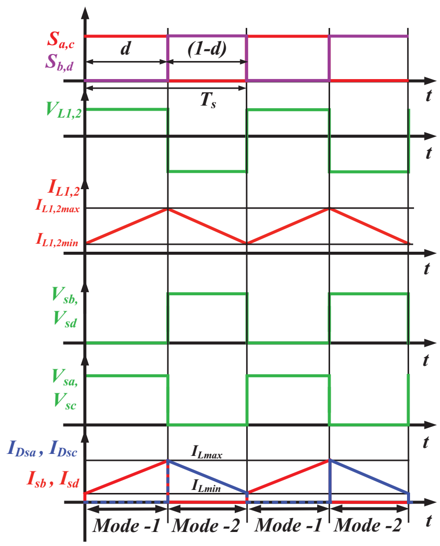

Fig. 3. Typical waveforms of the proposed NI-SIDO converter.

Mode-1: In this operational mode, the process of triggering switch S_b and S_d, with a gate signal is initiated. Inductor L_1 and L_2 commences linear charging via switch S_b and S_d, while capacitors C_1 and C_2 discharge through load. As a result, diode D_{sa} and D_{sb} shift into the "off" state. The equivalent circuit for this mode is depicted in Figure 2b. The inductor voltages, V_{L1} and V_{L2} and the capacitor currents i_{c1} and i_{c2} is given as below:

$$\begin{cases} V_{L1} = V_1 - i_{L1} r_{L1} \\ V_1 = i_{L_1} r_{L1} + L_1 \frac{di_{L1}}{dt} \\ i_{c1} = i_{o1} \end{cases} \tag{1}$$

where r_{L1} and r_{L2} represents the DC resistance of the inductors.

$$\begin{cases} V_{L2} = V_1 - i_{L2} r_{L2} \\ V_1 = i_{L_2} r_{L2} + L_2 \frac{di_{L2}}{dt} \\ i_{c2} = i_{o2} \end{cases} \tag{2}$$

Mode-2: When the gate pulses for switch S_b and S_d are removed, they transition into the "off" state. As a result, the voltage across the inductor causes diodes D_{sa} and D_{sc} to become forward-biased. The equivalent circuit for this mode is depicted in Figure 2c. During this mode, both the inductor and the source supply power to the load, and the inductor charges the capacitor. Consequently, an LC tank is formed in this mode. In this mode, the current through inductor L_1 and L_2 reaches its minimum values I_{L1min} and I_{L2min}. The voltage across inductors L_1 and L_2 and the current through capacitors C_1 and C_2 are as follows.

$$\begin{cases} V_{L1} = (V_1 - V_{o1}) - i_{L1} r_{L1} \\ (V_1 - V_{o1}) = i_{L1} r_{L1} + L_1 \frac{di_{L1}}{dt} \\ i_{c1} = i_{o1} - i_{L1} \end{cases} \tag{3}$$

This mode ends at the switching period T. The gating pulse continues to operate the converter in the above modes in the boost mode of operation.

B. Steady State Analysis

The steady-state analysis is done by considering the following assumptions: (i) the converter always operates in continuous conduction mode, and (ii) trace resistances are neglected. By accounting for the presence of parasitic components during both the "on" and "off" conditions, the steady-state analysis is presented in the section. The terms r_{c1},r_{c2} r_{L1},r_{L2},r_{on1} and r_{on2} are the parasitics of the capacitor, inductors, and switches. Here all the switches, inductors, and capacitors are of the same values, thus all these values are assumed as equal. So,$r_{c1} = r_{c2} = r_c$,$r_{L1} = r_{L2} = r_L$,$r_{on1} = r_{on2} = r_{on}$ are considered in the further analysis. The d is the on interval of the switches S_b and S_d and T_s is the time period, and f_s is the switching frequency.

During the on period, the voltage across the inductors is given by:

$$\begin{cases} V_{L1} = L_1 \frac{di_{L1}}{dt} = V_1 - (r_{on} + r_L) I_{L1} \\ V_{L2} = L_2 \frac{di_{L2}}{dt} = V_1 - (r_{on} + r_L) I_{L2} \end{cases} \tag{4}$$

During the off period, the voltage across the inductors is given by:

$$\begin{cases} V_{L1} = V_1 - \frac{V_{o1}}{\alpha_1} - \left(\frac{r_c}{\alpha_1} + r_L\right) I_{L1} + \left(\frac{r_c}{\alpha_1}\right) I_{o1} \\ V_{L2} = V_1 - \frac{V_{o2}}{\alpha_2} - \left(\frac{r_c}{\alpha_2} + r_L\right) I_{L2} + \left(\frac{r_c}{\alpha_2}\right) I_{o2} \end{cases} \tag{5}$$

where,

$$\begin{cases} \alpha_1 = \frac{R_{o1} + r_c}{R_{o1}} \\ \alpha_2 = \frac{R_{o2} + r_c}{R_{o2}} \end{cases} \tag{6}$$

The voltage gain of the proposed converter is obtained by applying the volt-second balance principle. Applying the volt-second balance principle in the inductors L_1 and L_2,

$$\frac{1}{T_s}\left[\int_0^d V_{L1} dt + \int_d^{T_s} V_{L1} dt\right] = 0 \tag{7}$$

From the equations in 5, gain can be obtained as

$$\begin{cases} V_{o1} = \frac{\alpha_1 V_1 - (\frac{r_c}{\alpha_1}(1-d) + r_L + r_{on} d)\alpha_1 I_{L1} + r_c(1-d) I_{o1}}{(1-d)} \\ V_{o2} = \frac{\alpha_2 V_1 - (\frac{r_c}{\alpha_2}(1-d) + r_L + r_{on} d)\alpha_2 I_{L2} + r_c(1-d) I_{o2}}{(1-d)} \end{cases} \tag{8}$$

where the d is the on interval of the switches S_b and S_d and T_s is the time period, and f_s is the switching frequency.

Considering the ideal conditions, the voltage gain equation (8) can be rewritten as,

$$\begin{cases} V_{o1} = \frac{V_1}{(1-d)} \\ V_{o2} = \frac{V_1}{(1-d)} \end{cases} \tag{9}$$

The inductor value is obtained by considering the inductor ripple current at 10%,

$$\begin{cases} L_{1min} \geq \frac{(V_{o1}-V_1)(1-d)}{\Delta i_{L1} f_s} \\ L_{2min} \geq \frac{(V_{o2}-V_1)(1-d)}{\Delta i_{L2} f_s} \end{cases} \tag{10}$$

Choosing the L value is taken as 5mH.

The capacitor value is obtained by considering the capacitor ripple voltage at 5%,

$$\begin{cases} C_{1min} \geq \frac{d}{R_{o1} \frac{\Delta V_{o1}}{V_{o1}} f_s} \\ C_{2min} \geq \frac{d}{R_{o2} \frac{\Delta V_{o2}}{V_{o2}} f_s} \end{cases} \tag{11}$$

Choosing the C value is taken as 150μF.

III. Results and Discussions

A. Simulation Results

The simulation of the newly designed NI-SIDO converter is conducted through MATLAB/Simulink software. Within the Simulink environment, a PV panel block is created using the design equations [19] and is utilized as the source V_1. To achieve output voltage regulation, a PI-based closed-loop controller is selected due to its enhanced stability and straightforward design. The controller operates by comparing the actual value of the output voltage of the converter with the reference voltage provided. The resulting error signal is then passed through the controller, as illustrated in Fig. 4. Simulation parameters are shown in the Table I.

TABLE I
Specifications of Simulation Model f_s = 10kHz

Parameter	Value
No: of cells	60
Parallel string	10
Series string	1
V_{mp}	20V
I_{mp}	5A
Inductors, L_1 & L_2	5mH
Capacitors, C_1 & C_2	150μF
Load Voltages	32V
Load Power	85W - 250W

The proposed converter is simulated using the MATLAB SIMULINK model. The simulation is conducted at 10kHz switching frequency. The results agreed with the theoretical values.

The loads are connected in parallel and are considered equal, so the inductors and capacitors chosen are also equal. The fig.5 are the results obtained from the simulation of the proposed system at constant irradiance with voltage mode control. The input voltage is kept at 24V with equal loads. From the figure, it can be seen that the load voltage at different loads, from 85W - 250W is varied but load voltages V_{O1} & V_{O2} is constantly maintained at 32V. These values are in agreement with the design equations in section 2.

Fig.7 are the results obtained from the simulation of the proposed system at constant irradiance with current mode control. The input voltage is kept at 24V. From the figure, it

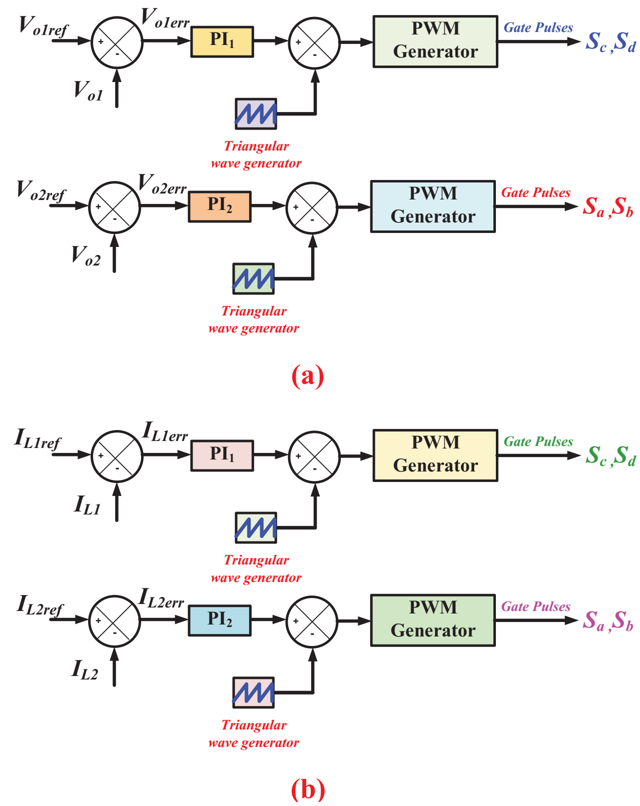

Fig. 4. Controller block diagram of a) Voltage mode control b) Current mode control

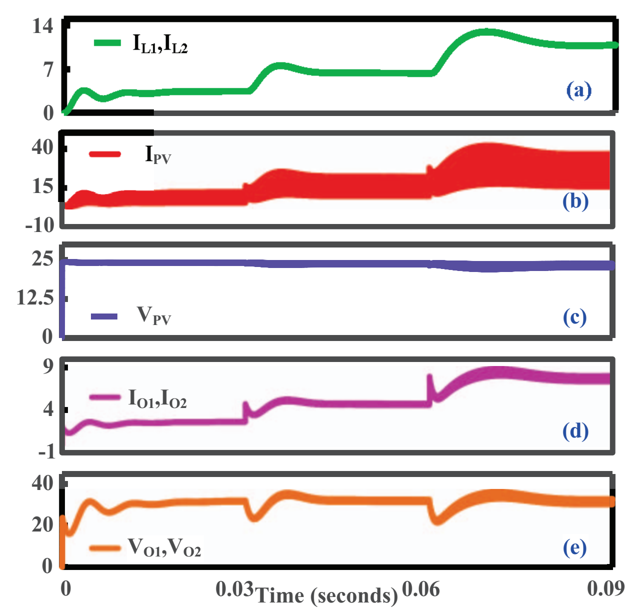

Fig. 5. Simulation results of solar PV input with irradiance at 1000W/m^2 a)I_{L1} , I_{L2} b) I_{PV} c) V_{PV} d) I_{O1} , I_{O2} e) V_{O1} , V_{O2} in voltage mode control

TABLE II
COMPARISON OF PROPOSED NI-SIDO CONVERTER WITH OTHER SIMILAR TOPOLOGIES

Parameter	[14]	[15]	[20]	[21]	NI-SIDO
No: of Switches	2	2	1	4	4
No: of Diodes	3	1	3	4	0
No: of Inductor	2	3	1	1	2
No: of Capacitor	3	3	3	2	2
Total count of components	10	9	8	11	8
No: of output ports	2	2	2	2	2
Input voltage	12V	12V	12V	18V,22V	24V
Output voltages	7.5V,29V	9V,16V	24V,48V	8V,12V	48V
Bidirectional	NO	NO	NO	NO	YES
Load Power	150W	18W,32W	38W,72W	-	75W,75W

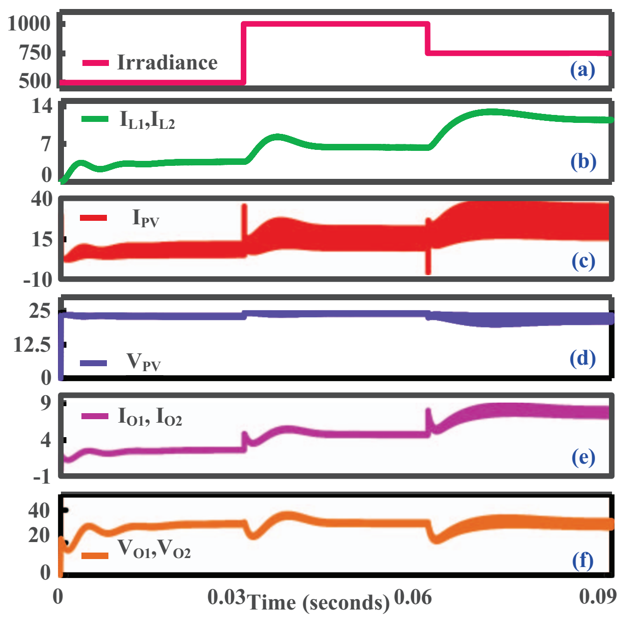

Fig. 6. Simulation results of solar PV input with a) varying irradiance b)I_{L1} , I_{L2} c) I_{PV} d) V_{PV} e) I_{O1} , I_{O2} f) V_{O1} , V_{O2} in voltage mode control

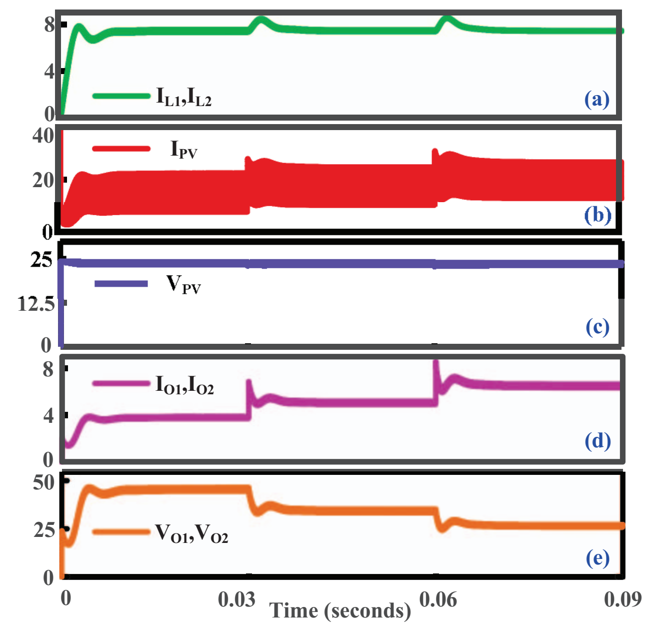

Fig. 7. Simulation results of solar PV input with irradiance at 1000W/m^2 a)I_{L1} , I_{L2} b) I_{PV} c) V_{PV} d) I_{O1} , I_{O2} e) V_{O1} , V_{O2} in current mode control

can be seen that the inductor currents I_{L1} & I_{L2} at different loads, from 85W - 250W are varied but load voltage I_L is constantly maintained at 7.4A. These values are in agreement with the design equations in section 2.

Fig.6 and Fig.8 represent the simulation results obtained with various irradiance levels from 500W/m^2-1000W/m^2 in 200W/m^2. The real-time testing of the proposed converter is performed using the OPAL-RT system, OP4510 for 48V. The results are presented in Fig.9, which shows the output voltage of 12*4 = 48V as a gain factor of 4 should be multiplied, as the DOUT of OPAL-RT is limited to -/+16V.

Table II illustrates the comparison of the proposed SIDO converter with other existing similar topologies. The proposed converter has fewer components even though it is a bidirectional converter with dual output.

IV. CONCLUSION

A NI-SIDO converter is proposed in the paper. The converter is designed and analyzed for equal outputs, 32V each. Real-time testing was conducted with the help of OPAL-RT, system, OP4510 for an output voltage level of 48V each. The conversion gain of the proposed converter is 1/(1-d). The simulation results of the proposed converter are presented for various scenarios such as at constant and variable irradiance for voltage mode control and current mode control is presented. The converter is capable of operating in a wide range of voltages. The results for separated looped voltage mode control and current model control of the interleaving are presented. It also shows the reduced capacitor voltage, which eliminated the use of a filter capacitor. In future work, the bi-directionality will be investigated.

REFERENCES

[1] P. Yang, C. K. Tse, J. Xu, and G. Zhou, âSynthesis and analysis of double-input single-output DC/DC converters,â IEEE Trans. Ind. Elec tron., vol. 62, no. 10, pp. 6284â6295, Oct. 2015.

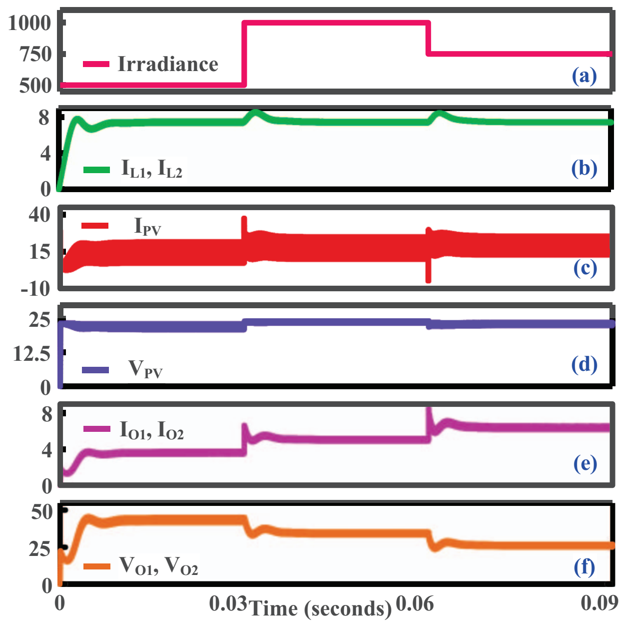

Fig. 8. Simulation results of solar PV input with a) varying irradiance b)I_{L1} , I_{L2} c) I_{PV} d) V_{PV} e) I_{O1}, I_{O2} f) V_{O1} , V_{O2} in current mode control

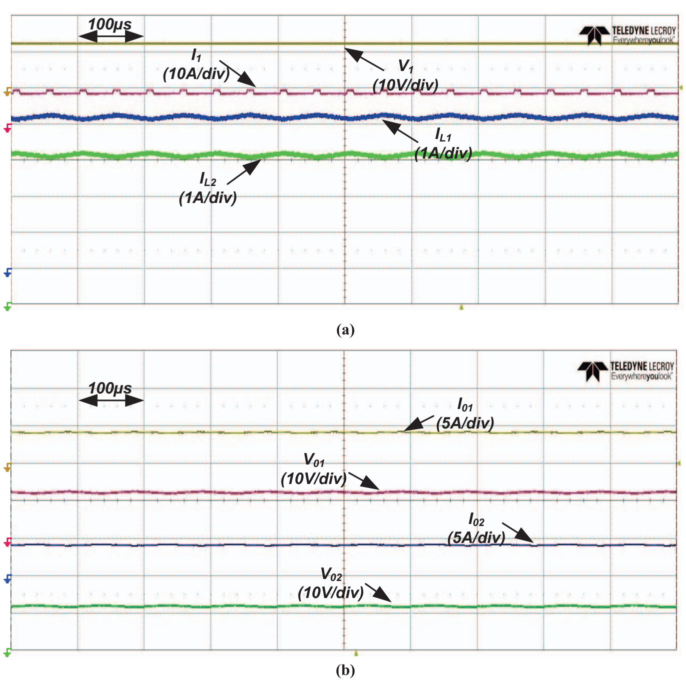

Fig. 9. Hardware results of proposed converter a)input voltage V_1, input current I_1 and inductor currents I_{L1} and I_{L2}, b) I_{O1} V_{O1}, I_{O2} V_{O2}

[2] Vijayan, M., et. al (2024). Dynamic Operation of Islanded DC Microgrid with Fuel Cell Using Hybrid Energy Storage Systems. In: Mahajan, V., Chowdhury, A., Singh, S.N., Shahidehpour, M. (eds) Emerging Technologies in Electrical Engineering for Reliable Green Intelligence. ICSTACE 2023. Lecture Notes in Electrical Engineering, vol 1117. Springer, Singapore. https://doi.org/10.1007/978-981-99-9235-5_18

[3] S. K. Kim, J. H. Jeon, C. H. Cho, J. B. Ahn, and S. H. Kwon, âDynamic modeling and control of a grid-connected hybrid generation system with versatile power transfer,â IEEE Trans. Ind. Electron., vol. 55, no. 4, pp. 1677â1688, Apr. 2008.

[4] Vijayan M, et. al. Optimal PI-Controller-Based Hybrid Energy Storage System in DC Microgrid. Sustainability. 2022 Nov 8;14(22):14666..

[5] S. Saggini and P. Mattavelli, âPower management in multi-source multi load energy harvesting systems,â in Proc. IEEE 13th Eur. Power Electron. Appl. Conf., 2009, pp. 1â10.

[6] J. Cao and A. Emadi, âA new battery/ultracapacitor hybrid energy storage system for electric, hybrid, and plug-in hybrid electric vehicles,â IEEE Trans. Power Electron., vol. 27, no. 1, pp. 122â132, Jan. 2011.

[7] Narasimharaju, B.L., Ramanjaneya Reddy, U. and Dogga, R., 2018. Design and analysis of voltage clamped bidirectional DCâDC converter for energy storage applications. The Journal of Engineering, July 2018, pp.367-374

[8] Y. Tong, Z. Shan, J. Jatskevich, and A. Davoudi, âA nonisolated multiple input multiple-output DCâDC converter for DC distribution of future energy efficient homes,â in Proc. 40th Annu. Conf. IEEE Ind. Electron. Soc., 2014, pp. 4126â4132.

[9] Raveendhra, Dogga, Rached Dhaouadi, Habibur Rehman, and Shayok Mukhopadhyay. "LC impedance source bi-directional converter with reduced capacitor voltages." Electronics 9, no. 7 (2020): 1062.

[10] Y. Tong, Z. Shan, C. N. M. Ho, and J. Jatskevich, âConcept of synthesizing modular power supply for interfacing diverse energy sources and loads,â in Proc. IEEE 16th Workshop Control Model. Power Electron., 2015, pp. 1â5.

[11] Vijayan M, Udumula RR, Mahto T. Comparative Study of Various DC-DC Converter Topologies for PV Powered EV Charging Stations. ECS Transactions. 2022 Apr 24;107(1):709.

[12] Khasim SR, Dhanamjayulu C, Muyeen SM. A Single Inductor Multi-Port Power Converter for Electric Vehicle Applications. IEEE Access. 2023 Jan 4;11:3367-85.

[13] H. Radmanesh and M. Rahimi, "A Common Ground Dual-Output Quasi-Z-Source DC-DC Converter," 2019 27th Iranian Conference on Electrical Engineering (ICEE), Yazd, Iran, 2019, pp. 570-575, doi: 10.1109/IranianCEE.2019.8786412.

[14] B. Faridpak, M. Farrokhifar, M. Nasiri, A. Alahyari and N. Sadoogi, "Developing a super-lift luo-converter with integration of buck converters for electric vehicle applications," in CSEE Journal of Power and Energy Systems, vol. 7, no. 4, pp. 811-820, July 2021, doi: 10.17775/CSEEJPES.2020.01880.

[15] L. Senapati, A. K. Panda, M. M. Garg and R. K. Lenka, "An Adaptive Estimator Based Sliding Mode Control of Nonisolated Single-Input Double-Output Cuk Converter," in IEEE Journal of Emerging and Selected Topics in Industrial Electronics, vol. 4, no. 2, pp. 482-491, April 2023, doi: 10.1109/JESTIE.2022.3224883.

[16] LitrÃ¡n, Salvador P., Eladio DurÃ¡n, Jorge SemiÃ£o, and Cristian DÃaz-MartÃn. "Multiple-output DCâDC Converters: Applications and solutions." *Electronics* 11, no. 8 (2022): 1258.

[17] Lindiya, S.A.; Subashini, N.; Vijayarekha, K. "Cross Regulation Reduced Optimal Multivariable Controller Design for Single Inductor DCâDC Converters." Energies 2019, 12, 477.

[18] Li, X.L.; Dong, Z.; Tse, C.K. "Complete family of two-stage singleinput multi-output configurations of interconnected power converters." IEEE Trans. Power Electron. 2020, 35, 3713â3728.

[19] Z. Li, S. Dusmez, and H. Wang, âA novel soft-switching secondary-side modulated multi-output dc/dc converter with extended zvs range,â IEEE Transactions on Power Electronics, 2018.

[20] Y. Ye and K. W. E. Cheng, âSingle-switch single-inductor multi-output pulse width modulation converters based on optimized switched capacitor,â IET Power Electronics, vol. 8, no. 11, pp. 2168â2175, 2015.

[21] B. Wang, X. Zhang, J. Ye, and H. B. Gooi, âDeadbeat control for single inductor multiple-input multiple-output dc-dc converter,â IEEE Transactions on Power Electronics, 2018